Using Redundancy in Serial Planar Mechanisms to Improve Output-Space Tracking Accuracy

S. Ambike[1], J.P. Schmiedeler[2] and M.M. Stanišić[2]

[1]*The Ohio State University, Columbus, Ohio, USA; e-mail: ambike.1@osu.edu*
[2]*University of Notre Dame, Notre Dame, Indiana, USA;*
e-mail: {schmiedeler.4,stanisic.1}@nd.edu

Abstract. Path tracking using planar mechanisms with one degree of redundancy can be enhanced by matching (when possible) or approximating second-order path properties with first-order joint coordination. Second-order tracking can reduce the frequency of feedback for the desired accuracy, and since this paper provides analytical expressions for the joint speed ratios, this advantage comes at no additional computational cost. Examples show that tracking solutions with this method are locally more accurate compared to unweighted pseudoinverse solutions. Therefore, the feedback frequency for a desired tracking accuracy can be reduced, potentially resulting in a reduced computational cost of path tracking.

Key words: Geometric tracking, speed-ratio control, redundancy resolution, planar mechanisms.

1 Introduction

Redundant manipulators are increasingly employed in useful practical tasks that are specified in terms of a geometric path to be followed by the end-effector. Redundant degrees of freedom make it possible to achieve objectives such as avoiding collisions, joint limits and/or singular configurations. However, objective criteria need to be specified to resolve the kinematic redundancy. Kinematic performance metrics, such as locally bounded joint-space velocities, involve computation of damped least-squares solutions [1], although such pseudoinverse-based control cannot avoid singular configurations [2]. Alternatively, time-optimal control uses the manipulator dynamics to minimize the performance time, which is a solved problem for non-redundant manipulators [3]. For kinematically redundant manipulators, numerical procedures have been proposed in [4] to achieve path-constrained time-optimal control. A computationally efficient feedback-control law is developed in [5] that provides joint forces/torques for a redundant manipulator while minimizing the output-space tracking error. These methods use information from the output-space path up to the first-order only, whereas the definition of the desired output-space path contains more geometric information in the form of higher order derivatives. Effective utilization of this path information can reduce the required feedback fre-

J. Lenarčič and M.M. Stanišić (eds.), *Advances in Robot Kinematics: Motion in Man and Machine*, DOI 10.1007/978-90-481-9262-5_15, © Springer Science+Business Media B.V. 2010

quency for a desired tracking accuracy and potentially, the computational cost of path tracking.

In [6], a curvature-theory-based approach is developed that maps the first- and second-order information of the output-space path onto the first- and second-order geometric properties of the joint space path for non-redundant, planar mechanisms. This method is extended to using the third-order path properties of constant curvature output-space paths in [7]. Recently, this approach has been generalized to path tracking with spatial, non-redundant systems using the geometric properties of the output-space path up to any order [8]. The present work illustrates how this approach, termed speed-ratio (SR) control, can be effectively applied to redundant, planar manipulators. It resolves kinematic redundancy by including higher-order geometric information from the desired path into the problem formulation. The resulting system of polynomial equations has analytical solutions for planar, three-degree-of-freedom (DOF) mechanisms, making this method computationally efficient.

The remainder of this paper is organized as follows. Section 2 describes the SR paradigm. Section 3 develops the application of SR control to three-DOF planar manipulators. Section 4 presents numerical examples. Section 5 gives conclusions.

2 Speed-Ratio Control for Non-Redundant Manipulators

The SR approach to control non-redundant mechanisms, developed in [8], is briefly described here. A trailing subscript(s) for a quantity indicates derivative with respect to the subscript(s), and a zero after the subscript(s) indicates that the derivative has been evaluated in the zero position. For example,

$$\bar{r}_{\theta_1} := \frac{d\bar{r}}{d\theta_1}, \quad \bar{r}_{\theta_1\theta_2 0} := \left.\frac{d^2\bar{r}}{d\theta_1 d\theta_2}\right|_0 .$$

The zero position is defined by the initial increments in the joint variables all being zero.

The geometric path tracking approach involves a reparameterization of the forward kinematic map of a tracking mechanism using the displacement of one joint, called the *leading joint*, as the independent variable. Motion of the other joints are related to that of the leading joint via Taylor series, the constants of which are called *speed ratios*. The jth-order speed ratio relating the motion of joint i to that of the leading joint when evaluated in the zero position is denoted by $n_i^{(j)}$. For $j = 1$, the superscript is omitted. Therefore,

$$n_3^{(3)} := \left.\frac{d^3\theta_3}{d\theta_1^3}\right|_0 \quad \text{and} \quad n_2^{(1)} := n_2 = \left.\frac{d\theta_2}{d\theta_1}\right|_0 .$$

For a d-DOF, non-redundant mechanism ($d = 2$ for planar and 3 for spatial systems), let θ_i denote the joint variables. Without loss of generality, the joint motions are coordinated using θ_1 as the leading joint:

$$\theta_i = n_i\theta_1 + \frac{1}{2!}n_i^{(2)}\theta_1^2 + \frac{1}{3!}n_i^{(3)}\theta_1^3 + \cdots \qquad i = 2, \cdots d. \tag{1}$$

The path $\overline{r}$ generated by the controlled point on the end effector (EE) is expressed as a function of θ_1 as

$$\overline{r}(\theta_1) = \overline{r}_0 + \overline{r}_{\theta_1 0}\theta_1 + \frac{1}{2!}\overline{r}_{\theta_1\theta_1 0}\theta_1^2 + \frac{1}{3!}\overline{r}_{\theta_1\theta_1\theta_1 0}\theta_1^3 + \cdots, \tag{2}$$

where $\overline{r}_0$ is the initial EE position, and $\overline{r}_{\theta_1 0} = \overline{r}(n_i)$, $\overline{r}_{\theta_1\theta_1 0} = \overline{r}(n_i, n_i^{(2)})$, and so on for higher order derivatives. Equation (1) allows the forward kinematics of the manipulator to be expressed as a curve in the output space parameterized in terms of θ_1, given by Eq. (2). The kinematics can be similarly characterized in terms of the arc length. However, arc-length parameterization fails for singular poses of the mechanism, whereas the present parameterization allows accurate geometric tracking even for singular poses [6]. The generated path is described by a Frenet-Serret (FS) frame, the components of which are defined by the vector terms in Eq. (2). For example, the tangent of the frame is parallel to $\overline{r}_{\theta_1 0}$, and the normal is parallel to $\overline{r}_{\theta_1\theta_1 0}$. Note that this description involves the unknown speed ratios. The geometry of the desired path is also described using a FS frame, but in this case, all of the quantities defining the frame are known. Control of the EE path geometry is achieved by matching the geometric properties of the frames describing the generated and desired paths. For example, matching the first-order geometric property means forcing the tangent of $\overline{r}(\theta_1)$ to be parallel to the tangent of the desired path. The resulting *coordination equation* is solved for the first-order speed ratios. Each higher order of geometry matching yields coordination equations that can be solved for the speed ratios of the corresponding order. The coordination equations for the first two orders are [8]

$$\overline{r}_{\theta_1 0} \times \hat{T} = \overline{0}, \tag{3}$$

$$\overline{r}_{\theta_1\theta_1 0} \times \hat{T} + \kappa_d(\overline{r}_{\theta_1 0} \cdot \overline{r}_{\theta_1 0})\hat{B} = \overline{0}, \tag{4}$$

where $\hat{T}$ and $\hat{B}$ are the tangent and binormal of the FS frame and κ_d is the curvature. Note that as control of path geometry is achieved, the corresponding geometric properties of the FS frames for the desired and generated paths become identical, and it becomes unnecessary to explicitly distinguish between them. Equation (3) can be solved for n_2 and n_3, Eq. (4) gives $n_2^{(2)}$ and $n_3^{(2)}$, and so on. Matching pth-order geometric properties yields the pth-order speed ratios. Equations (1) and (2) then determine the motion of the EE.

3 Speed-Ratio Control for Three-DOF, Planar Manipulators

For redundant mechanisms, assuming that the pose is non-singular, there will exist a family of joint-velocity solutions that achieve first-order tracking. A unique solution from this set can be chosen based on higher-order geometric information of the desired path. The order of the geometric properties that can be used to make this choice is generally determined by the order of joint control and the degree of redundancy in the system. For example, with first-order joint coordination, or joint-velocity control as is assumed in this paper, a three-DOF system can use second-order path properties, and a four-DOF system can use second- and third-order path properties. By applying the coordination equations to the redundant system, a set of polynomial equations is obtained that provide insight into the tracking capabilities of the mechanism and, for a three-DOF mechanism, provide analytical solutions for the best possible second-order tracking performance. In contrast, a *non-redundant*, planar mechanism must use second-order joint coordination to track path curvature, and accurate curvature tracking is ensured for non-singular mechanism poses.

For a general, planar three-DOF system, let θ_1, θ_2, and θ_3 be the joint variables. The leading joint is θ_1, and n_2 and n_3 are the two first-order speed ratios. Equation (3) provides one linear equation, and Eq. (4) provides one quadratic equation in the two unknown speed ratios.

$$A_1 n_2 + A_2 n_3 + A_3 = 0, \tag{5}$$

$$B_1 n_2^2 + B_2 n_3^2 + B_3 n_2 n_3 + B_4 n_2 + B_5 n_3 + B_6 = 0, \tag{6}$$

where the coefficients A_i and B_i are functions of the desired path tangent and the mechanism's geometry and current pose. Since Eq. (4) is linear in the desired curvature κ_d, a univariate polynomial can be obtained from Eqs. (5) and (6).

$$\Omega(n_2) := (a_1\kappa_d + b_1)n_2^2 + (a_2\kappa_d + b_2)n_2 + (a_3\kappa_d + b_3) = 0, \tag{7}$$

where the coefficients a_i and b_i are derived from A_i and B_i, and so they are also functions of the desired tangent and the mechanism geometry and pose. The curvature κ_d can be accurately matched if Eq. (7) has real solutions, the condition being,

$$\Delta := \left(a_2^2 - 4a_1a_3\right)\kappa_d^2 + \left(2a_2b_2 - 4a_1b_3 - 4b_1a_3\right)\kappa_d + \left(b_2^2 - 4b_1b_3\right) \geq 0. \tag{8}$$

By explicit calculation, it can be shown that for three-DOF planar mechanisms of all possible morphologies, the function $a_2^2 - 4a_1a_3 = 0$. Therefore,

$$\Delta = \kappa_d C + D, \tag{9}$$

where $C = 2a_2b_2 - 4a_1b_3 - 4b_1a_3$, and $D = b_2^2 - 4b_1b_3$. Note that κ_d is positive by definition. Therefore, if C and D are both positive, Δ is also positive for any κ_d. In this case, two solutions are obtained from Eqs. (7) and (5). The rate of change in curvature of the desired path can be used to choose from these two solutions, as illustrated in the numerical example in the following section. If $\Delta < 0$, the curvature cannot be matched exactly. In this case, the tracked curvature is treated as a variable, denoted by κ. The discriminant in Eq. (9) is now a function of κ, and a value $\kappa = \kappa_t$ can be obtained from the condition in Eq. (8) such that Eq. (7) yields real roots for n_2. If C and D are not both negative, the solution to the equation $\Delta(\kappa) = 0$ gives a positive generated curvature $\kappa_t = -\frac{D}{C}$, such that the error $|\kappa_t - \kappa_d|$ is minimum. The minimality condition is ensured by the continuity and monotonicity of $\Delta(\kappa)$.

When $C, D < 0$, the range of κ for which the condition in Eq. (8) is satisfied is given by $-\frac{D}{C} \geq \kappa$. Only negative values for κ are possible, indicating that the mechanism can only move along the desired tangent such that the normal vector of the generated path is in the opposite direction of the normal of the desired path. In this case, the generated path with the *smallest curvature magnitude* (the path with the greatest radius) will be the most accurate. Therefore, the smallest negative $\kappa_t = -\frac{D}{C}$ that satisfies the condition in Eq. (8) is the solution.

In conclusion, with first-order joint coordination, a three-DOF mechanism can track a desired path with a given curvature κ_d if the quantity Δ in Eq. (9) is greater than zero, and the speed ratios can be obtained from Eqs. (7) and (5). If $\Delta < 0$, the *best possible* generated path has curvature $\kappa_t := -\frac{D}{C}$. This solution can be substituted into Eq. (7) to obtain n_2, following which, Eq. (5) yields the value of n_3.

The three-prismatic manipulator is an exception to the above scheme. For this manipulator, C and D are zero, and the function Ω in Eq. (7) vanishes. This is a (perhaps intuitive) result indicating that the EE cannot move along curved paths with constant joint velocities for a three-DOF Cartesian robot, and therefore, path curvature cannot be tracked with first-order joint control.

The technique described here is applicable in principle to larger planar systems as well as spatial systems. However, the analyticity is quickly lost, since the size of the polynomial equations becomes large. For example, for a four-DOF, planar system employing first-order joint control, the first-, second-, and third-order coordination equations will be linear, quadratic, and sextic equations in three variables, respectively. A search algorithm must be employed to obtain real solutions for all three equations. This is a limitation of the approach. However, a useful result will be the characterization of the solution for the curvature-tracking problem before solving the full system. This is a subject of future work.

4 Examples

A 3-revolute (3R) mechanism has link lengths l_i, and θ_{i0} denote the initial values of the joint variables that define the zero position. Joint angle θ_{i0} is measured counterclockwise from link l_{i-1} to link l_i. The joint angle θ_{10} is measured with respect to a fixed reference axis. Two examples are provided, one with a positive value for the discriminant Δ, and the second with a negative value for Δ.

Example 1: Positive Δ
The link lengths are $l_1 = 1.15$, $l_2 = 1.5$, and $l_3 = 1.8$ in arbitrary length units. The initial pose, or zero position, is defined by $\theta_{10} = -14°$, $\theta_{20} = -10°$, and $\theta_{30} = -205°$.

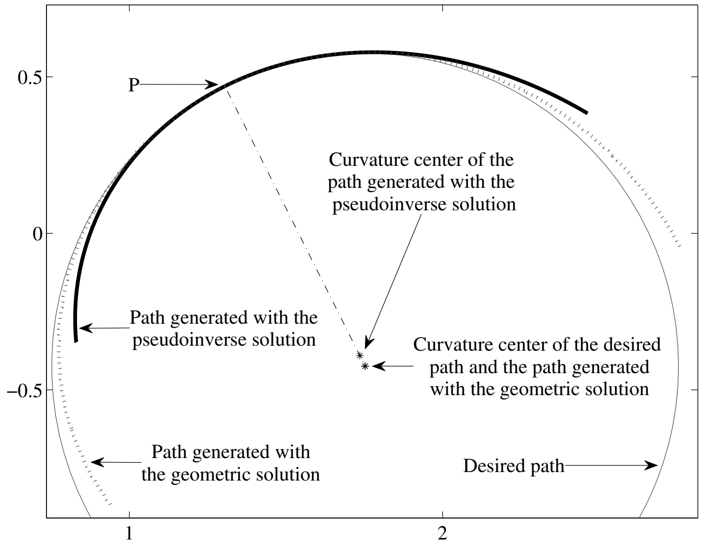

Fig. 1 The planar 3R mechanism is required to track the circular arc passing through point *P*. The dashed curve is the geometric tracking solution. The solid curve is the pseudoinverse tracking solution. Curvature centers for the three paths are shown. Only the curvature centers of the desired path and the path generated with the geometric solution match.

The desired path is a circular arc passing through the controlled point on the EE, point P. The desired tangent is $\hat{T} = [0.8944 \quad 0.4472 \quad 0]^T$, and κ_d is 1. Also, the rate of change of curvature is zero. The joint variable θ_1 is chosen as the leading joint variable. These system parameters yield constants A_i, a_i and b_i:

$$\begin{bmatrix} A_1 \\ A_2 \\ A_3 \end{bmatrix} = \begin{bmatrix} 0.2345 \\ 1.4247 \\ 0.0485 \end{bmatrix}, \quad \begin{bmatrix} a_1 \\ a_2 \\ a_3 \end{bmatrix} = \begin{bmatrix} -6.4670 \\ -26.3920 \\ -26.9267 \end{bmatrix}, \quad \begin{bmatrix} b_1 \\ b_2 \\ b_3 \end{bmatrix} = \begin{bmatrix} 6.7015 \\ 27.8167 \\ 26.9752 \end{bmatrix}.$$

This gives $C = -48.6844$, $D = 50.6686$, and $\Delta = 1.9842$. Therefore, Eqs. (5) and (7) provide two solutions for the speed ratios: $\{n_2 = -0.0343, n_3 = 3.0319\}$, and $\{n_2 = -6.0402, n_3 = -3.7154\}$. The first solution has a rate of change of curvature of -0.8262, and the second solution has a rate of change of curvature of 0.4414. Since the latter value is closer to the desired value 0, the second solution is chosen.

Alternative first-order speed ratios obtained as ratios of the joint velocities from the Jacobian pseudoinverse are $\{n_2 = 2.9052, n_3 = 6.3343\}$. Note that the norm of the pseudoinverse solution will be lower than the norm of the geometric solution once the EE-velocity magnitudes for both solutions are made equal by proper choice of the leading joint velocity. In Fig. 1, the EE paths generated by implementing the chosen geometric solution and the pseudoinverse solution are plotted until the position error, defined as the minimum distance of the EE from the desired path, reaches 0.025. Clearly, superior tracking accuracy is achieved by implementing speed-ratio

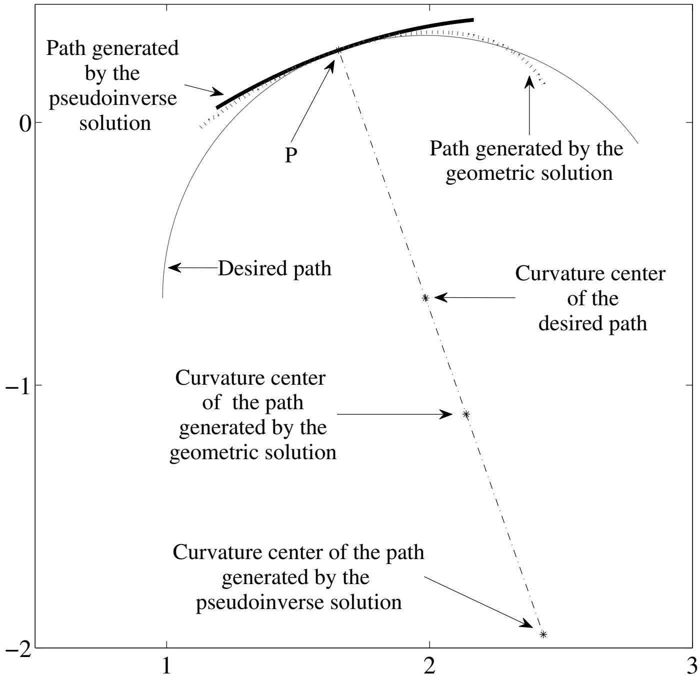

Fig. 2 The planar 3R mechanism is required to track the circular arc passing through point *P*. The dashed curve is the geometric tracking solution, and the solid curve is the pseudoinverse tracking solution. The curvature centers of the three paths are shown.

control. The EE path obtained from the geometric solution follows the desired path more closely and stays close to the desired path for a longer portion of the desired path compared to the pseudoinverse solution.

Example 2: Negative Δ

The zero position of the mechanism in the previous example is redefined by $\theta_{10} = -14°$, $\theta_{20} = -40°$, and $\theta_{30} = -205°$. The desired path is a circular arc passing through point P with tangent $\hat{T} = [0.9439 \quad 0.3304 \quad 0]^T$ and κ_d is 1. The rate of change in curvature is zero. The joint variable θ_1 is chosen as the leading joint variable. The constants A_i, a_i and b_i are

$$\begin{bmatrix} A_1 \\ A_2 \\ A_3 \end{bmatrix} = \begin{bmatrix} -9.6866 \\ -40.7486 \\ -42.8541 \end{bmatrix}, \quad \begin{bmatrix} a_1 \\ a_2 \\ a_3 \end{bmatrix} = \begin{bmatrix} -19.3305 \\ -102.2244 \\ -135.1469 \end{bmatrix}, \quad \begin{bmatrix} b_1 \\ b_2 \\ b_3 \end{bmatrix} = \begin{bmatrix} 3.4823 \\ 28.8917 \\ 49.2146 \end{bmatrix}.$$

This gives $C = -219.0375$, $D = 149.219$, and $\Delta = -69.8184$, indicating that the desired radius cannot be accurately matched. The tracked curvature is $\kappa_t = -\frac{D}{C} = 0.6812$, and the corresponding error is $|\kappa_d - \kappa_t| = 0.3188$. The geometric speed ratios are obtained by using the computed value of κ_t in Eqs. (7) and (5). The geometric and the pseudoinverse-based speed ratios, respectively, are $\{n_2 = -2.1033, n_3 = -0.7671\}$, and $\{n_2 = -0.7398, n_3 = -4.3965\}$. Figure 2 plots the paths generated by both solutions until the position error reaches 0.025. The curvature centers of neither solution match the desired curvature center. However, the curvature center obtained from the geometric solution is closer to the desired curvature center. Further, with first-order coordination, the curvature center of the generated path cannot be any closer to the desired curvature center given the tangent direction and the mechanism's pose. Therefore, the path obtained from the geometric solution is the most locally accurate path that can be achieved with first-order coordination.

5 Conclusions

Speed-ratio control is applied to resolve redundancy in path tracking with three-DOF planar mechanisms. Analytically obtained first-order joint motions minimize the difference between the curvatures of the generated and the desired output-space paths. Two examples are provided that compare the tracking performance of speed-ratio control with pseudoinverse solutions. The use of higher-order path information yields generated paths that track the desired path more closely. Less feedback will be required to achieve the desired tracking accuracy, and therefore, this method has the potential to reduce the computational cost of path tracking.

References

1. Chiaverini, S., Oriolo, G., Walker, I.A.D.: Kinematically redundant manipulators. In: Siciliano, B., Khatib, O. (Eds.), *Springer Handbook of Robotics*, Springer Verlag, pp. 245–268 (2008).
2. Baillieul, J., Hollerbach, J., Brockett, R.: Programming and control of kinematically redundant manipulators. In: *Proceedings of 23rd IEEE Conference on Decision and Control*, pp. 768–774 (1984).
3. Shin, K.G., McKay, N.D.: Minimum-time control of robotic manipulators with geometric path constraints, *IEEE Transaction on Automatic Control*, **AC 30**(6), 531–541 (1985).
4. Galicki, M.: Time-optimal control of kinematically redundant manipulators with geometric constraints. *IEEE Transactions on Robotics and Automation*, **16**(1), 89–93 (2000).
5. Galicki, M.: Adaptive control of kinematically redundant manipulator along a prescribed geometric path. In: Kozlowski, K. (Ed.), *Robot Motion and Control*, Springer, Berlin/Heidelberg, pp. 129–139 (2006).
6. Lorenc, S.J., Stanišić, M.M., Hall Jr. A.S.: Application of instantaneous invariants to the path tracking control problem of planar two degree-of-freedom systems: A singularity-free mapping of trajectory geometry, *Mech. Mach. Theory*, **30**(6), 883–896 (1995).
7. Lorenc, S.J., Stanišić, M.M.: Third-order control of a planar system tracking constant curvature paths, In: Lenarcic, J., Ravani, B. (Eds.), *Advances in Robot Kinematics and Computational Geometry*, Kluwer Academic Publishers, Dordrecht, pp. 229–238 (1994).
8. Ambike, S., Schmiedeler, J.P., Stanišić, M.M.: Geometric, spatial path tracking using non-redundant manipulators via speed-ratio control. In *Proceedings ASME International Design Engineering Technical Conferences & Computers and Information in Engineering Conference*, IDETC/CIE, to appear (2010).